Atmospheric NH₃ in urban Beijing: long-term variations and implications for secondary inorganic aerosol control

Ziru Lan[1], Xiaoyi Zhang[2], Weili Lin[1], Xiaobin Xu[2], Zhiqiang Ma[3], Jun Jin[1], Lingyan Wu[2], Yangmei Zhang[2]

5   [1]Key Laboratory of Ecology and Environment in Minority Areas, Minzu University of China, National Ethnic Affairs Commission, Beijing 100081, China
[2]Institute of Atmospheric Composition, Chinese Academy of Meteorological Science, Beijing 100081, China
[3]Institute of Urban Meteorology, China Meteorological Administration, Beijing 100089, China

Correspondence to: Weili Lin (linwl@muc.edu.cn)

10   **Abstract**

Ammonia (NH₃) has major effects on the environment and climate. In-situ measurements of NH₃ concentrations taken between June 2009 and July 2020 at an urban site in Beijing were analyzed to study its long-term behaviors, responses to meteorological conditions and influences on the formation of secondary inorganic aerosols (SIAs). The 11-year average NH₃ mixing ratio was 26.9 ± 19.3 ppb (median, 23.5 ppb). Annual average NH₃ mixing ratio increased from 2009 to 2017 by

15   50% and then decreased by 49% from 2017 to 2020. Notably, the long-term trend for NH₃ at the ground level did not align with the trends derived from satellite observations and emission estimates. The NH₃ concentration exhibited a stronger correlation with the daily variation in water vapor (H₂O) concentration than with air temperature. Thermodynamic modeling revealed the nonlinear response of SIAs to NH₃, with increased sensitivity when its concentration is reduced to 40% of the initial level. Although reducing NH₃ concentrations can improve air quality during winter, controlling acid gas

20   concentrations has a greater effect than controlling NH₃ concentrations on reducing SIA concentrations, until NH₃ and acidic gas concentrations are reduced below 80% of their current levels. Nevertheless, the increased mass proportion of ammonium salts in SIAs during the observation period indicates that future control measures for NH₃ concentrations may need to be prioritized in Beijing.
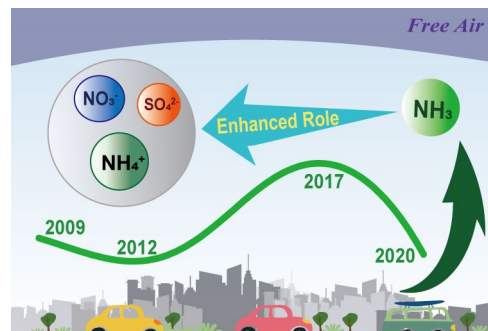
1 Introduction

Excessive input of anthropogenic nitrogen into the environment can directly harm ecosystems and influence climate change (Charlson et al., 1991; Reay et al., 2008; Shadman et al., 2016). As the most abundant alkaline trace gas in the atmosphere (Meng et al., 2017), NH_3 interacts with the oxidized products of atmospheric acidic gases to form secondary aerosols, which considerably affect the radiative balance of the atmosphere and air quality (Fuzzi et al., 2015). Over the years, China has been committed to controlling air pollution and has effectively managed the emissions of primary pollutants such as sulfur dioxide (SO_2) and nitrogen oxide (NO_x). However, particulate matter 2.5 ($PM_{2.5}$, particulate matter with a diameter less than 2.5 μm in size) pollution is still a severe problem. Existing studies on controlling SO_2 and NO_x emissions indicate that controlling NH_3 emissions is the most economically effective way for reducing $PM_{2.5}$ concentrations (Gu et al., 2021; Pinder et al., 2008; Xie et al., 2022). However, the effectiveness of NH_3 reduction varies by region (Liu et al., 2019b; Karydis et al., 2021), and there is still a debate regarding the efficacy of NH_3 reduction measures (Guo et al., 2018; Meng et al., 2022; Wei and Mohamed Tahrin, 2023).

Anthropogenic sources are the primary contributors to atmospheric NH_3 emission (Olivier et al., 1998). In China, agricultural sources dominate, accounting for approximately 80% of total emissions (Zhou et al., 2015). However, the contribution of non-agricultural sources in urban areas is considered significant. Studies indicate that over 30% of NH_3 emissions observed in urban areas can be attributed to traffic (Elser et al., 2018; Gu et al., 2022a; Walters et al., 2022). Nevertheless, some research suggests that biogenic sources (primarily green spaces) predominate in urban and account for approximately 60% of emissions (Teng et al., 2017), while the contribution from traffic sources is negligible (Yao et al., 2013). The complexity of urban NH_3 sources results in intricate variability in its atmospheric characteristics.

Long-term observations are important for analyzing the environmental impacts and control strategies of atmospheric NH_3. In Europe (Horváth and Sutton, 1998; Sutton et al., 2001; Horvath et al., 2009; den Bril et al., 2011; Lolkema et al., 2015; Tang et al., 2018), North America (Butler et al., 2016; Yao and Zhang, 2019; Yamanouchi et al., 2021) and Asia (Yamamoto et al., 1995, 1988; Saraswati et al., 2017), studies have been conducted on NH_3 variations over a period of 5 years or more. In most of these regions, NH_3 concentrations have either remained stable or have exhibited an increasing trend. Satellite observations detected rising global atmospheric NH_3 concentrations, influenced by reductions in acidic gas emissions, temperature increases and the rising use of chemical fertilizers (Warner et al., 2017). In China, according to the monitoring results from the Nationwide Nitrogen Deposition Monitoring Network (NNDMN), NH_3 concentrations at 12 urban sites and 43 rural sites increased by approximately 80% from 2011 to 2018 (Wen et al., 2020). Satellite data analysis by Dong et al. (2023) indicated a significant increase (~32%) in NH_3 vertical column densities in China from 2008 to 2019. In the North China Plain, a hotspot for global NH_3 emissions, Luo et al. (2020) found a rapid increase in urban NH_3 concentration from 2011 to 2018. Wen et al. (2024) found a 26% decrease in Beijing NH_3 concentrations from August 2005 to August 2020, and a 50% increase from January 2005 to January 2020. Currently, long-term ground-based observations of atmospheric NH_3 at

high temporal resolution are relatively rare in China, and the contrasting trends between NH_3 emissions, satellite and in-situ measured concentrations in urban areas have not been fully explored.

The present study examined high temporal resolution NH_3 observations at the surface in urban Beijing from 2009 to 2020. Using data from emission inventories, satellite observations, meteorological elements, concentrations of various types of atmospheric pollutants, and particle ion composition, the present study aimed to obtain the characteristics of long-term variations, influencing factors, and the contributions of NH_3 to particle formation in the atmosphere of Beijing. Analyzing long-term NH_3 observations helps to understand how changes in NH_3 concentrations have affected atmospheric pollution in the past. This knowledge is crucial for predicting future atmospheric pollution and formulating effective environmental policies. Furthermore, it provides a scientific basis and reference for developing future NH_3 control strategies.

2 Materials and methods

2.1 Data

Between June 2009 and July 2020, data on continuous online measurements of NH_3 concentrations were collected in Haidian District, Beijing (39°95'N, 116°32'E, Figure S1). From June 2009 to September 2017, data were collected from an observational site located on the third floor of a building within the premises of the China Meteorological Administration (CMA). Subsequently, the observation site was relocated to the 14th floor of the Science and Technology Building of Minzu University of China (MUC), which was less than 1 km away from the previous location and located just across the road from it. The ground-floor elevations of both buildings are 56 m above sea level, and the observation heights above the ground are 10 m on the 3rd floor and 56 m on the 14th floor. Both observation sites were surrounded mostly by urban roads, office spaces, residential areas, and parks, and no large-scale industrial sources of NH_3 were located near the site.

Beginning in June 2009, NH_3 concentration monitoring was conducted using an EC9842 NO_x/NH_3 Analyzer (Ecotech, Australia). Starting in April 2015, additional NH_3 measurements were simultaneously taken using an EAA NH_3 Analyzer (Los Gatos Research, USA). From May 2016 onward, only the EAA NH_3 Analyzer was used. The EC9842 NO_x/NH_3 Analyzer employs gas-phase chemiluminescence to continuously analyze NH_3, NO_x, and N_x concentrations; its detection limit is less than 2 ppb and data record time is 1 minute. The instrument was subject to weekly zero and span checks to identify potential analyzer faults and response drift. Multipoint calibrations were typically performed every month, and data were corrected on the basis of the multipoint calibrations. The EAA NH_3 Analyzer features a low detection limit of less than 0.2 ppb and a maximum drift of 0.2 ppb within 24 hours, with a time resolution of 50 seconds, and it utilizes Off-Axis Integrated Cavity Output Spectroscopy technology. At CMA site, the air had been drained into an air-conditioned room with a 4.5 m long Teflon line, and the inlet height is 1.8 m above the rooftop (about 12 m above ground level). At MUC site, air is introduced from outside the sealed window through a borehole, with the air inlet extending 20-30 cm outside the window.

Since it is on the 14th floor, the air outside the building flows smoothly. To maintain data comparability, NH_3 standard gases, which had been traceable to a uniform standard, were used as measurement references. The comparison result of the two instruments can be found in Zhang et al. (2021), in which the two instruments exhibited a considerable correlation, with a correlation coefficient of 0.949 (n = 5316, p < 0.01) and slope of s 0.999 ± 0.005.

During data analysis, minute-level data were converted into hourly average data. Throughout the observation period, a total of 40,692 and 46,917 valid hourly average data points were obtained from the EC9842 and EAA analyzers, respectively, resulting in a total of 13,420 data sets being obtained simultaneously through measurements on the two instruments. These two sets of results exhibited a significant correlation (N = 13,420, slope = 1.09, R = 0.95, p < 0.05), and the parallel observations from the two analyzers were generally consistent (Figure S2). The NH_3 observation data were finalized by averaging the synchronized data.

Furthermore, NH_3 satellite observation data were obtained through Metop-A satellite's Infrared Atmospheric Sounding Interferometer (IASI) remote sensing product. These data had a spatial resolution of 12×12 km^2 and were collected monthly (Van Damme et al., 2017). In the present study, daytime satellite NH_3 data from June 2009 to April 2020 were used. The average NH_3 satellite observation results for Beijing were calculated using data for the region spanning 36.5°N to 42.5°N in latitude and 113.5°E to 118.5°E in longitude. The trend for satellite observation values obtained at the grid point at the location of the monitoring station closely matched the trend for the average observation values collected for this region (Figure S3). NH_3 emission inventory data for Beijing (from June 2009 to December 2017) were presented in Figure S4, comparing NH_3 emissions from Beijing and its surrounding areas (Huang et al., 2012; Kang et al., 2016). Meteorological data collected between June 2009 and February 2012 were obtained from the Beijing Capital International Airport station. From March 2012 to April 2020, meteorological data were sourced from the Haidian Meteorological Station. The temperature and relative humidity data acquired from the two stations exhibited a high level of correlation (Figure S5). Absolute humidity was calculated using the acquired temperature and relative humidity data. Data for other pollutants such as $PM_{2.5}$, SO_2, and NO_2 were acquired from the Wanliu Monitoring Station in Haidian District, Beijing. These monitoring data were collected between April 2, 2014, and July 11, 2020. Figure S6 provides additional details of these data.

In the present study, offline sampling of $PM_{2.5}$ was conducted on the rooftop of the School of Pharmacy at Minzu University in China. Atmospheric samples were collected twice daily, specifically from 6:00 to 17:00 (daytime sampling) and from 18:00 to 5:00 on the following day (nighttime sampling). The sampling periods were from September 8 to 21, 2018 (autumn); November 6 to 21, 2018 (autumn); January 1 to 21, 2019 (winter); March 3 to 21, 2019 (spring); May 8 to 15, 2019 (spring); and June 8 to 21, 2019 (summer). The collected $PM_{2.5}$ samples on filters were subsequently sent to the Chinese Academy of Meteorological Sciences for chemical analysis of ion components (Na^+, SO_4^{2-}, NH_4^+, NO_3^-, Cl^-, Ca^{2+}, K^+, and Mg^{2+}), from which 184 data sets were obtained. Additionally, data from the study by Hu et al. (2014) that spanned from May 5 to November 30, 2009, and data from the study of Wu et al. (2019) that spanned December 15 to 23, 2016, were

used in the present study as references for monitoring $PM_{2.5}$ components within the premises of the China Meteorological Administration.

2.2 Data analysis methods

2.2.1 Long-term trends analysis

Long-term trends of atmospheric NH_3 were obtained using Ensemble Empirical Mode Decomposition (EEMD) (Wu and Huang, 2009). This method adaptively decomposes a signal into a series of Intrinsic Modal Functions (IMFs) from high to low frequencies. It separates oscillation or trend components of varying scales from the original signal. EEMD integrates the advantages of wavelet analysis and augments the Empirical Mode Decomposition (EMD) method by introducing white noise. This enhancement effectively mitigates the mode mixing problem inherent in the EMD method. EEMD demonstrates greater stability in decomposing nonlinear and non-stationary data series, enabling the accurate extraction of genuine signal variations (Qian et al., 2011). Currently, EEMD has been used in studies on air-quality trend analysis (Yao and Zhang, 2016; Fu et al., 2020; Wang et al., 2022; Wang and Zhang, 2023). In the present study, the EEMD was performed using the Rlibeemd package of the R programming language (Luukko et al., 2016).

2.2.2 Thermodynamic modeling

The ISORROPIA-II model is mainly used to simulate the physical state and concentration of inorganic components of the aerosol system at thermodynamic equilibrium. A distinct advantage of the ISORROPIA-II model over other thermodynamic models is the inclusion of the K^+, Ca^{2+}, and Mg^{2+} ions in the calculations, and taking these components into account significantly improves the accuracy of the model simulations (Allen et al., 2015). Additionally, the high precision and computational efficiency of the ISORROPIA II model have been widely demonstrated (Fountoukis and Nenes, 2007). To assess the sensitivity of sulfate, nitrate, and ammonium (SNA) to changes in precursor concentrations, the present study employed the ISORROPIA II thermodynamic equilibrium, version 2.3 (http://isorropia.epfl.ch). The model was run in "forward + metastable" mode, taking inputs such as temperature (in Kelvin), relative humidity (up to 1), and concentrations of particulate components (SO_4^{2-}, Cl^- + HCl, NO_3^- + HNO_3, NH_4^+ + NH_3, Na^+, K^+, Ca^{2+} and Mg^{2+}) expressed in $\mu g\ m^{-3}$ for calculations.

3 Results and discussion

3.1 Long-term variations in NH_3

From June 2009 to July 2020, the hourly average mixing ratio of atmospheric NH_3 in Beijing was 26.9 ± 19.3 ppb (median, 23.5 ppb). Table S1 summarizes results from various NH_3 monitoring studies conducted in urban areas. The results of the present study are basically consistent with the annual NH_3 mixing ratio averages that were observed in urban Beijing by

other researchers through optical instruments (Gu et al., 2022a, 2022b; Pu et al., 2020; Sun et al., 2023; Wang et al., 2019). As a densely populated country with intensive agriculture activities, China contains several areas that are major global hotspots for the atmospheric NH_3 concentration (Liu et al., 2019a; Van Damme et al., 2018). The monitoring results of the present study indicate that the overall NH_3 mixing ratio in Beijing is lower than that in Delhi (Saraswati et al., 2019; Singh and Kulshrestha, 2014) but considerably higher than those in other developed cities such as New York, Toronto, and Rome (Chatain et al., 2022; Nguyen et al., 2021; Park et al., 2021; Perrino et al., 2002; Phan et al., 2013; Zbieranowski and Aherne, 2012; Zhou et al., 2019). Even within China, the NH_3 mixing ratio in Beijing is higher relative to that in Shanghai, which is also a megacity (i.e., the NH_3 mixing ratio in Shanghai is less than one-third of that in Beijing), and only a few cities in North China have mixing ratios comparable to that in Beijing (Cao et al., 2009; Chang et al., 2019; Huang et al., 2021; Pan et al., 2018). The primary reasons for this phenomenon are the frequent agricultural activities and the presence of highly alkaline soils in the North China Plain, where Beijing is located (Ju et al., 2009).

Due to significant data gaps from January 2013 to June 2013 and from May 2017 to August 2017, the period from 2009 to 2020 was divided into three segments for linear regression analysis (Figure S7). From June 2009 to January 2013, the observed hourly average atmospheric NH_3 mixing ratio showed a decreasing trend (R = −0.23, p < 0.05, slope = −0.01); from June 2013 to May 2017, the NH_3 mixing ratio increased (R = 0.04, p < 0.05, slope = 0.22×10-2); and from September 2017 to July 2020, the NH_3 concentration exhibited a decreasing trend again (R = −0.03, p < 0.05, slope = −1.42×10^{-3}). Similar to in situ observations, the satellite observations of NH_3 concentration showed a decreasing trend from June 2009 to January 2013 (R = −0.19, p < 0.05, slope = −3.88×10^{-4}) and an increasing trend from June 2013 to May 2017 (R = 0.12, p < 0.05, slope = 3.65×10^{-4}), but differed from in situ atmospheric NH_3 trends as it continued to rise from September 2017 to July 2020 (R = 0.23, p < 0.05, slope = 1.17×10^{-3}).

To further analyze the long-term trends of the atmospheric NH_3 concentration, the present study referred to the findings of Vu et al. (2019) and used meteorological factors to construct a random forest model for imputing missing values. The computed time series for the atmospheric NH_3 concentration is presented in Figure S8. The complete dataset obtained through EEMD was used to characterize the changes in atmospheric NH_3 concentrations in Beijing (Figure 1). The NH_3 mixing ratio initially exhibited a slight decrease but started to increase in 2012 and peaked in 2017, subsequently declining. From 2009 to 2017, the NH_3 mixing ratio increased by 50%, but by 2020, the NH_3 mixing ratio had decreased by 49% from its peak in 2017. A comparison of monthly average NH_3 concentrations obtained from satellite observations revealed that prior to 2018, the trend for the surface NH_3 mixing ratio was similar to that observed by satellites, exhibiting a decline followed by an increase in atmospheric NH_3 concentrations. However, starting in 2018, these two trends diverged, with satellite observations indicating a continued increase in NH_3 concentrations, while the surface NH_3 mixing ratio exhibited a decreasing trend.The monitoring results of this study were compared with NH_3 monthly concentrations observed by NNDMN in Beijing from April 2011 to December 2015 (Xu et al., 2019) and from January 2005 to August 2020 (Wen et al.,

180   2024) (Figure S9). From April 2011 to December 2015, both the NH_3 mixing ratio observed in this study (R = 0.27, p < 0.05) and the satellite-observed concentrations (R = 0.28, p < 0.05) exhibited increasing trends, while the NNDMN station did not show a significant trend (R = 0.16, p > 0.05). The NNDMN station observations from January 2009 to August 2020 were significantly correlated with this study's observations (R_{Aug} = 0.66, p < 0.05; R_{Jan} = 0.65, p < 0.05), but neither the present study's observations nor the NNDMN observations were significantly correlated with satellite-observed NH_3

185   concentrations. Satellite observations showed a strong correlation between NH_3 concentrations in the Beijing urban area and the Beijing-Tianjin-Hebei region (Figure S3). However, measurements by Zhang et al. (2020) at five stations in Beijing indicated that four stations had lower NH_3 concentrations in 2017 (winter) than in 2020 (winter + spring), while one station had higher concentrations in 2017 than in 2020, indicating variability in observation results even within the same city. Due to the short atmospheric lifetime, low transport altitude, high dry deposition rate, limited transport distance, and abundance

190   of atmospheric NH_3, its complex temporal and spatial characteristics contribute to the complexity of NH_3 variations (Asman and van Jaarsveld, 1992; Nair and Yu, 2020). Satellite observations are limited by the observation height and spatial resolution, which may mask variations in local surface NH_3 concentrations. Additionally, differences between the present study's observations and satellite observations may also be due to changes in the monitoring location and observation height in September 2017. However, tower observations conducted by the Institute of Atmospheric Physics, Chinese Academy of

195   Sciences (6.7 km from the present study's site) in the urban area showed only slight variations within a 300 m altitude range (Wang et al., 2019; Zhang et al., 2019). Therefore, the change in observation altitude may have had a limited impact on the change in NH_3 mixing ratio trends after 2017.
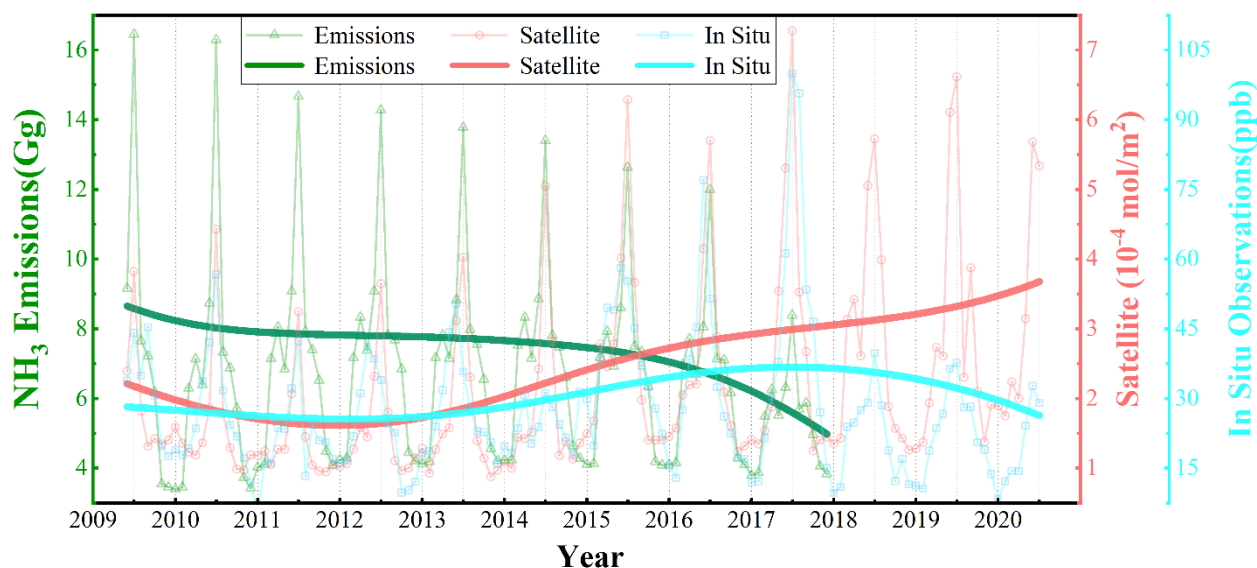
Figure 1: Monthly averages of surface observations and satellite inversions of NH_3 concentrations and total NH_3 emissions in
200   **Beijing from June 2009 to July 2020 (fine dotted line) and trends pertaining to changes (thick solid line).**

3.2 Influences on variation characteristics of NH₃

NH₃ emissions directly affect the variations in atmospheric NH₃ concentrations. The emission inventory data (Figure 1) indicate that NH₃ emissions in Beijing remained stable from 2009 to 2014, peaking in 2012. After 2014, NH₃ emissions in Beijing rapidly decreased, declining by 25% from 2014 to 2017. However, during this period of declining emissions, the NH₃ mixing ratio in Beijing exhibited an increasing trend. Similar phenomena have been reported by studies conducted outside of China. For instance, in Scotland, NH₃ emissions decreased by approximately 15% from 1990 to 2003, whereas atmospheric NH₃ concentrations increased (Friedman and Schwartz, 2011). In Hungary, NH₃ emissions were estimated to have decreased by 50% from 1983 to 1993; however, NH₃ concentrations exhibited a slight upward trend during this monitoring period (Horvath et al., 2009). A possible reason for these differences between NH₃ emissions and concentrations could be the significant reduction in the concentrations of SO_2 and NO_x, which reduced the amount of atmospheric NH₃ neutralized by acid gases (Fu et al., 2017; Lachatre et al., 2019; Liu et al., 2018; Yu et al., 2018). Over the past 2 decades, Beijing has implemented a series of strict measures to control air pollution and has achieved considerable success (United Nations Environment Programme, 2019). The concentrations of SO_2, NO_2, CO, PM_{10}, and $PM_{2.5}$ in Beijing all exhibited decreasing trends; in particular, the concentration of SO_2 decreased by 88% from 2009 to 2020 (Figure 2).
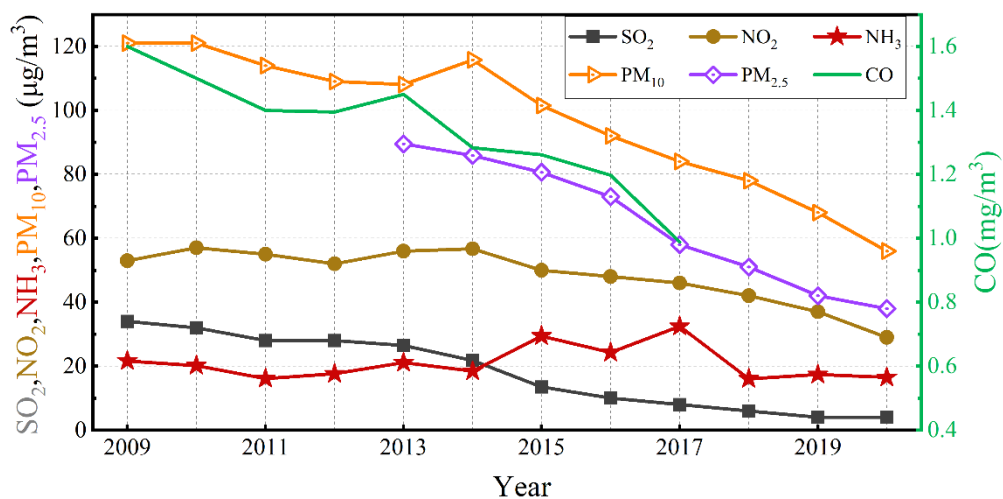
Figure2: Annual average concentrations of atmospheric NH₃ and six air pollutants in Beijing. The measurement unit is mg/m³ for CO concentration and µg/m³ for all other pollutants (air pollutant data were retrieved from the Beijing Environmental Bulletin website: http://sthjj.beijing.gov.cn/bjhrb/index/xxgk69/sthjlyzwg/1718880/1718881/1718882/).

To discuss the influence of chemical loss on the annual increase in NH_3 concentrations, the present study referred to research by Yao et al. (2019), assuming that NH_4^+ is uniformly distributed in the urban area of Beijing and that changes in NH_4^+ concentrations directly affect atmospheric NH_3 concentrations on a 1:1 basis. By calculating the change in NH_4^+ concentration relative to the baseline year, we adjust the atmospheric NH_3 concentrations. The present study set 2009 as the baseline year, using the annual average NH_4^+ concentration observed by Cheng (2021) in the urban area of Beijing to calculate the adjusted NH_3 concentrations from 2009 to 2017. The calculations show (Figure S10) that overall, the original NH_3 concentration in 2017 was 50% higher than in 2009, and the adjusted NH_3 concentration was 46% higher. Therefore, changes in chemical losses have a limited impact on the increased trend of NH_3 concentrations, and the discrepancy between NH_3 concentrations and emission trends may be due to imperfections in the emission inventory.

Various meteorological factors can influence the atmospheric NH_3 concentration. Among the identified factors, temperature has been reported to be positively correlated with the NH_3 concentration. An increase in temperature can increase soil NH_3 emissions, leading to the equilibrium shift of particulate NH_4NO_3 toward gaseous NH_3, which increases the NH_3 concentration (Behera et al., 2013; Li et al., 2014). During the observation period, the temperature in Beijing followed the seasonal sequence of summer (being the warmest), followed by spring, autumn, and winter, and the rankings of NH_3 mixing ratios across the seasons were consistent with the trend. Other studies conducted in temperate regions of the Northern Hemisphere have reported similar findings (Liu et al., 2021; Shon et al., 2012; Wang et al., 2018). The interannual trends for temperature and NH_3 mixing ratios across multiple seasons (Figure 3) revealed that temperature remained stable in summer and autumn over the years; when calculated in Kelvin, the average seasonal temperatures exhibited interannual variation coefficients of 0.42% in spring, 0.15% in summer, 0.17% in autumn, and 0.51% in winter. For the two seasons of summer and autumn, no significant correlation was identified between the annual average NH_3 mixing ratio and the variations in temperature over the years. After 2014, the annual average temperature in spring remained stable, whereas the NH_3 mixing ratio gradually decreased, possibly because of a reduction in agricultural activities. A weak positive correlation was identified between the annual average NH_3 mixing ratio and temperature only in winter, and the significant increase in winter temperature from 2013 to 2014 could have led to the high NH_3 mixing ratios in the winter of 2014.
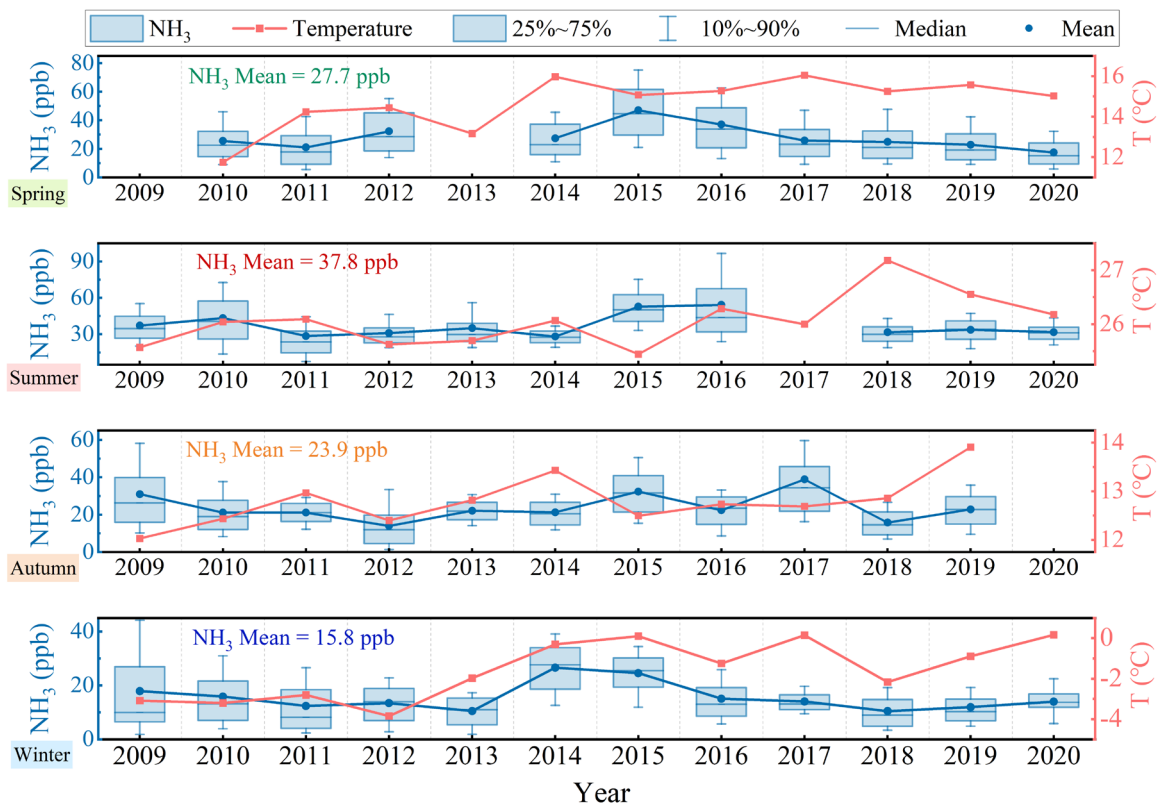
Figure 3: Interannual variations in mean NH₃ mixing ratio and mean temperature in Beijing for each season.

Our investigation examined the correlations among daily temperature, absolute humidity, and diurnal fluctuations of atmospheric NH_3 concentrations throughout an observation period of 4,058 days (screening criteria for effective dates: $p < 0.05$ and ≥ 18 effective hours per day, the p-values were adjusted using the Benjamini-Hochberg method (Benjamini and Hochberg, 1995)). We observed that temperature exhibited both positive (45%) and negative (55%) correlations with the NH_3 mixing ratio, with these two categories each accounting for nearly half of the valid observation days. However, on most days (i.e., 93% of the valid observation days), absolute humidity was positively correlated with the NH_3 mixing ratio (Figure S11). Overall, the average daily variations in NH_3 mixing ratios in Beijing in spring, summer, and autumn indicated a significant negative correlation with the temperature ($R_{spring} = -0.93$, $R_{summer} = -0.72$, $R_{autumn} = -0.76$, $p < 0.01$). The NH_3 mixing ratio was positively correlated with absolute humidity ($R_{spring} = 0.80$, $R_{summer} = 0.50$, $R_{autumn} = 0.67$, $R_{winter} = 0.49$, $p < 0.01$).

Several studies have suggested that temperature plays a pivotal role in driving diurnal variations in atmospheric NH_3 concentrations (Clarisse et al., 2021; Langford et al., 1992). However, the present study shows that NH_3 concentrations are significantly influenced by temperature across seasonal changes (Figure 3); in terms of diurnal patterns, the days showing

positive and negative correlations between NH$_3$ concentrations and temperature each constitute nearly half of the effective observation days (Figure S11). The mean diurnal variations in different seasons typically exhibit lower concentrations during the day and higher at night in spring, summer, and autumn (Figure S12). This difference suggests that correlations observed on a seasonal (climatic scale) tend to obscure lower-frequency data relationships, with daily variations in NH$_3$ concentrations being more influenced by the transition from day to night (meteorological or weather scale). This highlights the complex factors affecting NH$_3$ concentrations in the urban areas of Beijing and underscores the importance of high temporal resolution in observations. Several studies have noted a reduction in NH$_3$ concentrations during daylight hours (Buijsman et al., 1998; Sharma et al., 2014; Gu et al., 2022b; Lan et al., 2021). Increased temperatures during the day promote the volatilization of NH$_3$, but lower daytime concentrations may result from higher wind speeds and more favorable mixing conditions, whereas at night, NH$_3$ tends to accumulate within a shallower boundary layer (Buijsman et al., 1998). The diurnal variation of the boundary layer height in Beijing exhibits a single-peak pattern, rising rapidly from 6:00 to 8:00, reaching its peak between 14:00 and 15:00, then declining sharply, and stabilizing after 18:00 to 20:00 (Figure S12). During the daytime, NH$_3$ concentrations are influenced by a combination of temperature (which promotes emissions) and changes in the boundary layer height (which causes dilution), with the valley value of NH$_3$ concentrations lagging behind the peak times of boundary layer height and temperature. Moreover, during spring, summer, and autumn, the continuous decline in NH$_3$ concentrations during the daytime indicates that vertical mixing transport has a limited impact on atmospheric NH$_3$ in the urban areas of Beijing. In winter, the evaporation of dew or frost in the early morning leads to a rapid increase in H$_2$O and NH$_3$ concentrations (Wentworth et al., 2016), while the effects of afternoon temperature and vertical mixing dilution are comparable, keeping NH$_3$ concentrations relatively stable.

Several studies reported a high correlation between the NH$_3$ mixing ratio and humidity. Previous research has shown that NH$_3$ can be significantly affected only by sharp changes in humidity, and a new balance requires tens of minutes to be re-established. Averaging minute-level data over one hour can smooth the effects caused by variations in humidity. Notably, parallel observations in urban and suburban Beijing found that a positive correlation between daily NH$_3$ and H$_2$O concentration variations was only significant in urban areas (Lan et al., 2021). Gu et al. (2022b) reported daily variations in NH$_3$ concentrations in urban Beijing, as measured by the Picarro Ammonia Analyzer and ChemComb were consistent. These suggest that atmospheric NH$_3$ cannot be explained solely by the influence of H$_2$O effects on the instruments. Additionally, Sun et al. discovered a positive correlation between atmospheric NH$_3$ concentrations and relative humidity (RH) in Beijing and a negative correlation in Shanghai (Sun et al., 2023). In rural North China, He et al. (2020) also observed a strong correlation between NH$_3$ and RH, which they attributed to dew evaporation. At present, the relationship between the NH$_3$ mixing ratio and the water vapor concentration requires further clarification.

In summary, the results suggest that temperature plays a pivotal role in driving the seasonal variations in atmospheric NH$_3$ concentrations throughout a given year. However, in the long term, the influence of temperature and other meteorological

factors may be masked. Regarding diurnal variations, our analysis revealed that a single-day increase in temperature did not consistently lead to a direct elevation in atmospheric NH_3 mixing ratios on most days. Conversely, atmospheric water vapor mixing ratios exhibited a consistently positive correlation with NH_3 mixing ratios throughout the day. Notably, the day-to-day variations in meteorological factors remained consistent across the years, whereas the variation in diurnal NH_3 differed across different years and seasons (Figure S13). Therefore, the conclusion is that diurnal fluctuations in the atmospheric NH_3 concentration are not solely determined by meteorological factors. In recent years, scholars have been increasingly studying the contribution of traffic sources to urban NH_3 concentrations. Gu et al. (2022b) confirmed that vehicle exhaust emissions during winter in Beijing lead to the occurrence of morning peaks in NH_3 concentrations. Nonetheless, our results indicated that atmospheric NH_3 concentrations did not consistently peak in the morning throughout the observation period, even when high concentrations of traffic emissions were present. Furthermore, the morning peaks for atmospheric NH_3 concentrations tended to occur earlier relative to those for CO, which are influenced by traffic emissions (Figure S13).

Studies have comprehensively explored the influence of wind direction and wind speed on the pollutant mixing ratios in Beijing, and they have reported that southerly (S) winds transport a high concentration of pollutants to Beijing, leading to the accumulation of NH_3 in the city. Conversely, the winds from the north by west (NW) facilitate the dispersion and dilution of atmospheric NH_3 in Beijing (Lin et al., 2011; Meng et al., 2017). Figure S14 presents the wind rose diagrams for atmospheric NH_3 concentrations in various seasons and wind speeds. Under near-calm wind conditions (wind speed [ws] $\leq$ 1.5 m/s), the prevailing winds across all seasons were predominantly in the northeast and east-northeast directions, and NH_3 mixing ratios did not vary significantly because of the wind direction, indicating that local emissions had the most pronounced effect on atmospheric NH_3 concentrations. At low wind speeds (1.6 m/s $\leq$ ws $\leq$ 3.3 m/s), the predominant wind direction varied across seasons, with southwesterly winds prevailing in spring and summer and northerly winds dominating in autumn and winter. At higher wind speeds (ws > 3.4 m/s), the predominant wind direction was NW in spring, autumn, and winter but southerly in summer. In general, changes in the prevailing wind direction did not significantly influence NH_3 mixing ratios across various wind sectors. However, in specific wind sectors, such as the west by south (WS) sector in spring, the east by south (ES) sector in summer and autumn, and the south by east (SE) sector in winter, higher wind speeds tended to lead to lower NH_3 mixing ratios (Figure S15). Notably, the decline in NH_3 mixing ratios was more pronounced in wind sectors affected by NW winds, indicating that strong winds, particularly those from the NW direction, had a significant cleansing effect on NH_3 in Beijing. Conversely, southerly winds, and sometimes specific wind directions, contributed to NH_3 accumulation.

3.3 Influence of NH_3 on secondary inorganic aerosol formation

The present study investigated the role of atmospheric NH_3 in the formation of SIAs in Beijing by analyzing the relationship between NH_3 and SNA concentrations during the observation period. According to the study of Wei et al. (2023) conducted between 2013 and 2020, the SNA concentrations in Beijing exhibited a significant downward trend. However, the proportion

325 of SNA in PM$_{2.5}$ (mass concentration) did not change substantially during this period. Table S2 lists the proportions of various SNA components in PM$_{2.5}$ (mass concentration) recorded in urban areas of Beijing for the years 2009, 2016, 2018, and 2019. In the summer and autumn of 2009, SO$_4^{2-}$ accounted for more than 50% of SNA content, considerably exceeding the concentrations of NO$_3^-$ and NH$_4^+$. However, by 2016, except for the summer season when SO$_4^{2-}$ was still the predominant component, NO$_3^-$ became the dominant component of the SNA mass concentration. Over time, the proportion

330 of NH$_4^+$ in the SNA mass concentration increased across multiple seasons. Wen et al. (2024) and Cheng (2021) have also observed this phenomenon in urban Beijing. These findings indicate the necessity of controlling NH$_3$ and NO$_x$ concentrations to mitigate future PM$_{2.5}$ pollution.

Figure 4 depicts the relationship of NH$_4^+$ in fine particulates to atmospheric NH$_3$. Overall, a positive correlation was identified between NH$_4^+$ and NH$_3$, indicating that variations in the concentration of the precursor gas NH$_3$ influenced the

335 formation of NH$_4^+$. An increase in the NH$_3$ concentration led to a higher concentration of NH$_4^+$ in fine particulate matter, and this effect was most pronounced in winter, in which the correlation between NH$_4^+$ and NH$_3$ was the strongest (R^2 = 0.68, p < 0.01), and the average molar concentration ratio of NH$_4^+$ to NH$_3$ was the highest. The seasonal differences in the response of aerosol NH$_4^+$ on atmospheric NH$_3$ may mainly be caused by variations in meteorological conditions, in addition to those in precursor gases of SNA. For example, low temperature and high humidity promote the conversion of gaseous NH$_3$ to

340 particulate NH$_4^+$ (Wang et al., 2015). Thus, winter meteorological conditions may increase the formation of NH$_4^+$ in fine particulate matter, exacerbating fine particulate pollution and haze formation.
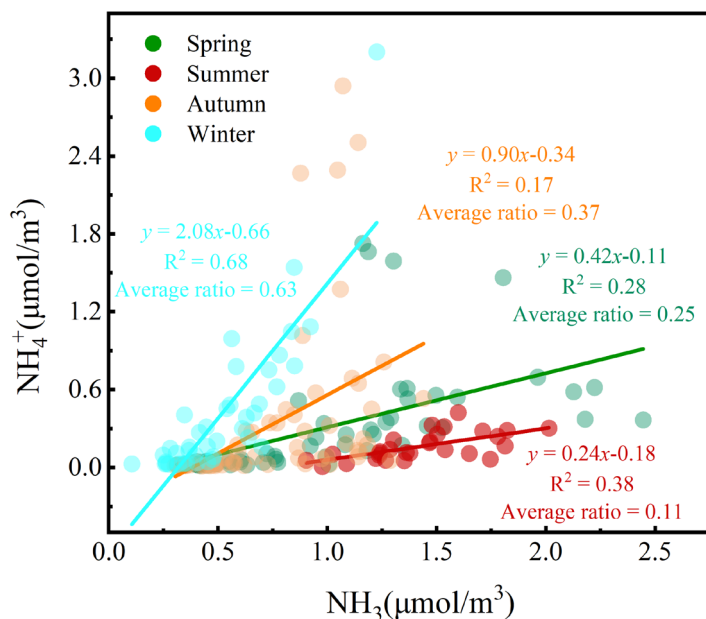
Figure 4: Correlation between gaseous NH$_3$ and fine particulate ion NH$_4^+$.

To gain further insights, the ISORROPIA II thermodynamic equilibrium model was employed to simulate and analyze the sensitivity of SNA in $PM_{2.5}$ to changes in precursor concentrations in each season. Concentrations of SO_4^{2-} + H_2SO_4 (TS), HNO_3 + NO_3^- (TN), and NH_3 + NH_4^+ (TA) were increased or reduced by up to 20%, and the changes in simulated concentrations relative to the baseline (without perturbation) were calculated. The simulation results revealed a strong correlation between the simulated and observed NH_3 concentrations (R_{spring} = 0.89, R_{summer} = 1.00, R_{autumn} = 0.97, R_{winter} = 0.98, $p < 0.01$), indicating the reliability of above observation-based results. The simulation results (Table S3) indicated that NH_4^+ was the least sensitive component to changes in the TA concentration in spring, autumn, and winter, suggesting that atmospheric NH_3 was not the limiting reactant for the generation of $(NH_4)_2SO_4$ and NH_4NO_3 in these seasons during the observation period. The responses of NH_4^+ to changes in TA and TN concentrations were less apparent in summer because NH_4^+ was mainly bound to SO_4^{2-} rather than to NO_3^- during this hot season, in which the high temperature was unfavorable for the generation and retention of NH_4NO_3. Furthermore, the increase in TS had an over or nearly (winter) proportional perturbation effect on NH_4^+, indicating the presence of sufficient NH_3 in the atmosphere of Beijing throughout the year. Su et al. (2021) also suggested that the acidic components in the atmosphere in Beijing were sufficiently neutralized. Therefore, a relatively smaller reduction (20%) in NH_3 abundance seems not to be able to significantly lower the SNA levels in Beijing.

When NH_3 was abundant, the sensitivity of SNA content to changes in TA within the ±20% range was low (within ±2%, Table S3). Under such conditions, changes in TS and TN concentrations had much larger perturbation effects on SNA concentrations. However, the winter SNA concentrations mostly responded linearly to changes in TS and TN concentrations but nonlinearly to changes in the TA ones (Figure 5). If the TA concentrations were reduced by 60%, the rate of decrease in SNA content would have accelerated considerably, which were more pronounced in 2019. By contrast, the effect of changes in the TS concentration decreased after its reduction of over 40%. In a previous study based on nationwide measurements and simulation, Meng et al. (2022) suggested that SNA content in China can be more effectively controlled by reducing the concentrations of acidic gases (SO_2 and NO_x) in the atmosphere than by reducing the concentration of NH_3 by the same percentage. Additionally, Zheng et al. (2022) discovered that the joint control of SO_2 and NO_x emissions is still the preferred method for reducing SNA concentrations in Central China, unless when acidic gas emissions are well controlled and the environmental chemical balance tends to favor the effective control of NH_3. Therefore, under the current atmospheric conditions, controlling acidic gas emissions is still a priority for reducing the $PM_{2.5}$ concentration in Beijing. Nevertheless, the cost of emissions reduction also increases with the progress of controlling SO_2 and NO_x emissions. Although they provide similar abatement benefits, the cost of reducing NH_3 is only 10% of that required to reduce NO_x (Gu et al., 2021). Thus, reducing NH_3 emissions should be prioritized as a means of improving future air quality in Beijing.
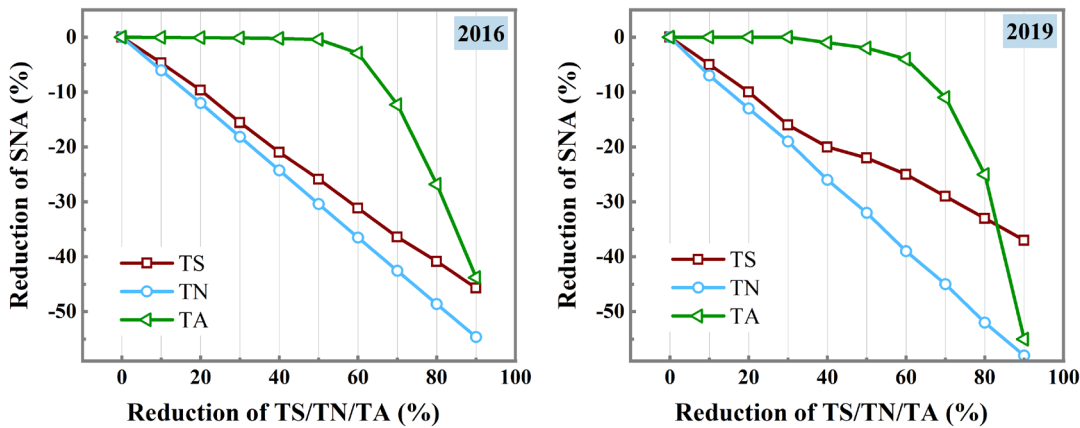
Figure 5: ISORROPIA predictions of percentage reduction in SNA mass concentration based on winter observations (charts display percentage reduction in SNA plotted against percentage reduction in TS, TN, and TA concentrations).

4 Conclusions

Over these 11 years, the NH_3 concentration in urban Beijing initially increased by 50% in the first 8 years but subsequently decreased by 49% in the following 3 years. In particular, the annual average concentration of NH_3 in 2020 was 24% lower than that in 2009. The trend for NH_3 mixing ratios did not align with those for annual NH_3 emissions and the increasing trend indicated by satellite-based NH_3 monitoring data. These discrepancies highlight the complexity of NH_3 sources and removal processes in urban areas, which implies further challenges of performing atmospheric NH_3–related modeling and implementing future emission reduction strategies.

The long-term trend in NH_3 in urban Beijing was not significantly influenced by meteorological factors such as temperature. However, the seasonal variations in NH_3 mixing ratios were strongly influenced by temperature, with higher temperatures corresponding to higher NH_3 mixing ratios during warmer seasons. Regarding daily variations, NH_3 mixing ratios exhibited both positive and negative correlations with temperature but consistently exhibited a positive correlation with absolute humidity on most days. Across the observation years, the daily variations in NH_3 concentrations did not exhibit a consistent pattern across different seasons. In some cases, the patterns were even entirely opposite. By contrast, various meteorological factors and the daily variation patterns of other common air pollutants were mostly consistent across different years and seasons. Consequently, the factors influencing atmospheric NH_3 concentrations appeared to be more complex compared with those influencing other common air pollutants.

The concentrations of various $PM_{2.5}$ ion components in Beijing for the years 2009, 2016, 2018, and 2019 indicate that, apart from the summer season, the SNA content in Beijing was mainly dominated by sulfate (nearly 50%). Furthermore, the

proportion of ammonium in SNA content increased over time. An analysis of the neutralization levels of major acidic gases and a modeling analysis of perturbation indicated that an excessive concentration of NH_3 was maintained throughout the year in Beijing. The findings of the present study suggest that even though the concentrations of SO_2 and NO_x in Beijing have decreased substantially over the past 2 decades, SIA formation is more sensitive to acid gases than to NH_3. Therefore,

400   reducing acidic gas emissions is still a primary focus for controlling fine particulate matter pollution in Beijing. Given that the trends in urban atmospheric NH_3 concentrations do not align with emissions trends, clarifying the relationship between them and identifying the sources of NH_3 in Beijing will play a crucial role in effectively reducing atmospheric NH_3 concentrations in the city.

In the present study, atmospheric NH_3 concentrations in urban Beijing were continuously monitored over a long period with

405   high temporal resolution. However, it should be noted that the potential limitations of surface monitoring in representing urban or regional trends due to the uneven distribution of atmospheric NH_3 sources and the lack of vertical information. Similarly, with monitoring at a single site, it is necessary to verify whether the response measures are broadly applicable across the entire Beijing urban area. This will require further observational research on atmospheric NH_3 in urban Beijing in the future. In addition, existing studies have demonstrated that emission inventories have underestimated atmospheric NH_3

410   emissions in the Beijing urban area (Xu et al., 2023), and the assessment results have varied across emission inventories (Chen et al., 2023). Additionally, given the limited research years of current emission inventories, the observed differences between long-term trends in monitored NH_3 concentrations and NH_3 emissions require continued attention in the future.

Data availability

For access to datasets, please contact Weili Lin.

415   **Author contributions**

Z. L., W.L., and X.X. designed the research, interpreted the data, and wrote the manuscript, Z.L., W.L., X.Z., Z.M. conducted the NH_3 measurements and J.J., Y.Z., L.W. contributed the ion component data in $PM_{2.5}$. The manuscript was written through the contributions of all authors. All authors have given approval to the final version of the manuscript.

Competing interests

420   The contact author has declared that none of the authors has any competing interests.

Acknowledgments

The authors are grateful for the assistance of colleagues for sample collection.

Financial support

This work was supported by the National Natural Science Foundation of China (grant no. 91744206, grant no. 42175128),
the Beijing Municipal Science and Technology Commission (grant no. Z181100005418016), and the CAMS technology and
development fund project (2022KJ005).

References

A review of 20 Years' Air Pollution Control in Beijing: http://www.unep.org/resources/report/review-20-years-air-pollution-control-beijing, last access: 20 June 2023.

Allen, H. M., Draper, D. C., Ayres, B. R., Ault, A., Bondy, A., Takahama, S., Modini, R. L., Baumann, K., Edgerton, E., Knote, C., Laskin, A., Wang, B., and Fry, J. L.: Influence of crustal dust and sea spray supermicron particle concentrations and acidity on inorganic NO_3^- aerosol during the 2013 Southern Oxidant and Aerosol Study, Atmos Chem Phys, 15, 10669–10685, https://doi.org/10.5194/acp-15-10669-2015, 2015.

Asman, W. A. H. and van Jaarsveld, H. A.: A variable-resolution transport model applied for NH_x in Europe, Atmospheric Environment. Part A. General Topics, 26, 445–464, https://doi.org/10.1016/0960-1686(92)90329-J, 1992.

Behera, S. N., Sharma, M., Aneja, V. P., and Balasubramanian, R.: Ammonia in the atmosphere: a review on emission sources, atmospheric chemistry and deposition on terrestrial bodies, Environ Sci Pollut R, 20, 8092–8131, https://doi.org/10.1007/s11356-013-2051-9, 2013.

Benjamini, Y. and Hochberg, Y.: Controlling the False Discovery Rate: A Practical and Powerful Approach to Multiple Testing, Journal of the Royal Statistical Society: Series B (Methodological), 57, 289–300, https://doi.org/10.1111/j.2517-6161.1995.tb02031.x, 1995.

Buijsman, E., Aben, J. M. M., Van Elzakker, B. G., and Mennen, M. G.: An automatic atmospheric ammonia network in the Netherlands set-up and results, Atmos. Environ., 32, 317–324, https://doi.org/10.1016/S1352-2310(97)00233-1, 1998.

Butler, T., Vermeylen, F., Lehmann, C. M., Likens, G. E., and Puchalski, M.: Increasing ammonia concentration trends in large regions of the USA derived from the NADP/AMoN network, Atmos Environ, 146, 132–140, https://doi.org/10.1016/j.atmosenv.2016.06.033, 2016.

Cao, J.-J., Zhang, T., Chow, J. C., Watson, J. G., Wu, F., and Li, H.: Characterization of Atmospheric Ammonia over Xi'an, China, Aerosol Air Qual Res, 9, 277–289, https://doi.org/10.4209/aaqr.2008.10.0043, 2009.

Chang, Y., Zou, Z., Zhang, Y., Deng, C., Hu, J., Shi, Z., Dore, A. J., and Collett, J. L.: Assessing Contributions of Agricultural and Nonagricultural Emissions to Atmospheric Ammonia in a Chinese Megacity, Environ Sci Technol, 53, 1822–1833, https://doi.org/10.1021/acs.est.8b05984, 2019.

Charlson, R. J., Langner, J., Rodhe, H., Leovy, C. B., and Warren, S. G.: Perturbation of the northern hemisphere radiative balance by backscattering from anthropogenic sulfate aerosols, 43, 152, https://doi.org/10.3402/tellusb.v43i4.15404, 1991.

Chatain, M., Chretien, E., Crunaire, S., and Jantzem, E.: Road Traffic and Its Influence on Urban Ammonia Concentrations (France), Atmosphere-basel, 13, 1032, https://doi.org/10.3390/atmos13071032, 2022.

Chen, J., Cheng, M., Krol, M., de Vries, W., Zhu, Q., Liu, X., Zhang, F., and Xu, W.: Trends in anthropogenic ammonia emissions in China since 1980: A review of approaches and estimations, Frontiers in Environmental Science, 11, https://doi.org/10.3389/fenvs.2023.1133753, 2023.

Chen, S., Cheng, M., Guo, Z., Xu, W., Du, X., and Li, Y.: Enhanced atmospheric ammonia (NH_3) pollution in China from 2008 to 2016: Evidence from a combination of observations and emissions, Environ Pollut, 263, 114421, https://doi.org/10.1016/j.envpol.2020.114421, 2020.

Cheng Mengtian: Long-term Trends in the Concentration of Water-Soluble Inorganic Salts in Beijing's Atmosphere and Their Response to Policy, PhD, Lanzhou University, https://doi.org/10.27204/d.cnki.glzhu.2021.000098, 2021. (Chinese)

Clarisse, L., Damme, M., Hurtmans, D., Franco, B., Clerbaux, C., and Coheur, P.: The Diel Cycle of NH_3 Observed From the FY‐4A Geostationary Interferometric Infrared Sounder (GIIRS), Geophys Res Lett, 48, e2021GL093010, https://doi.org/10.1029/2021gl093010, 2021.

den Bril, B. V., Meremans, D., and Roekens, E.: A Monitoring Network on Acidification in Flanders, Belgium, The Scientific World Journal, 11, 2358–2363, https://doi.org/10.1100/2011/897308, 2011.

Dong, J., Li, B., Li, Y., Zhou, R., Gan, C., Zhao, Y., Liu, R., Yang, Y., Wang, T., and Liao, H.: Atmospheric ammonia in China: Long-term spatiotemporal variation, urban-rural gradient, and influencing factors, Science of The Total Environment, 883, 163733, https://doi.org/10.1016/j.scitotenv.2023.163733, 2023.

Elser, M., El-Haddad, I., Maasikmets, M., Bozzetti, C., Wolf, R., Ciarelli, G., Slowik, J. G., Richter, R., Teinemaa, E., Hüglin, C., Baltensperger, U., and Prévôt, A. S. H.: High contributions of vehicular emissions to ammonia in three European cities derived from mobile measurements, Atmos. Environ., 175, 210–220, https://doi.org/10.1016/j.atmosenv.2017.11.030, 2018.

Fountoukis, C. and Nenes, A.: ISORROPIA II: a computationally efficient thermodynamic equilibrium model for K^+–Ca^{2+}–Mg^{2+}–NH_4^+–Na^+–SO_4^{2-}–NO_3^-–Cl^-–H_2O Aerosols, Atmos Chem Phys, 7, 4639–4659, https://doi.org/10.5194/acp-7-4639-2007, 2007.

Friedman, M. and Schwartz, A. J.: Monetary Trends in the United States and the United Kingdom: Their Relations to Income, Prices, and Interest Rates, University of Chicago Press, Chicago, IL, 696 pp., 2011.

Fu, H., Zhang, Y., Liao, C., Mao, L., Wang, Z., and Hong, N.: Investigating PM2.5 responses to other air pollutants and meteorological factors across multiple temporal scales, Sci Rep-uk, 10, 1–10, https://doi.org/10.1038/s41598-020-72722-z, 2020.

Fu, X., Wang, S., Xing, J., Zhang, X., Wang, T., and Hao, J.: Increasing Ammonia Concentrations Reduce the Effectiveness of Particle Pollution Control Achieved via SO_2 and NO_X Emissions Reduction in East China, Environ Sci Tech Let, 4, 221–227, https://doi.org/10.1021/acs.estlett.7b00143, 2017.

Fuzzi, S., Baltensperger, U., Carslaw, K., Decesari, S., Denier van der Gon, H., Facchini, M. C., Fowler, D., Koren, I., Langford, B., Lohmann, U., Nemitz, E., Pandis, S., Riipinen, I., Rudich, Y., Schaap, M., Slowik, J. G., Spracklen, D. V., Vignati, E., Wild, M., Williams, M., and Gilardoni, S.: Particulate matter, air quality and climate: lessons learned and future needs, Atmos Chem Phys, 15, 8217–8299, https://doi.org/10.5194/acp-15-8217-2015, 2015.

Gu, B., Zhang, L., Van Dingenen, R., Vieno, M., Van Grinsven, H. J., Zhang, X., Zhang, S., Chen, Y., Wang, S., Ren, C., Rao, S., Holland, M., Winiwarter, W., Chen, D., Xu, J., and Sutton, M. A.: Abating ammonia is more cost-effective than nitrogen oxides for mitigating PM 2.5 air pollution, Science, 374, 758–762, https://doi.org/10.1126/science.abf8623, 2021.

Gu, M., Pan, Y., Sun, Q., Walters, W. W., Song, L., and Fang, Y.: Is fertilization the dominant source of ammonia in the urban atmosphere?, Science of The Total Environment, 838, 155890, https://doi.org/10.1016/j.scitotenv.2022.155890, 2022a.

Gu, M., Pan, Y., Walters, W. W., Sun, Q., Song, L., Wang, Y., Xue, Y., and Fang, Y.: Vehicular Emissions Enhanced Ammonia Concentrations in Winter Mornings: Insights from Diurnal Nitrogen Isotopic Signatures, Environ Sci Technol, 56, 1578–1585, https://doi.org/10.1021/acs.est.1c05884, 2022b.

Guo, H., Otjes, R., Schlag, P., Kiendler-Scharr, A., Nenes, A., and Weber, R. J.: Effectiveness of ammonia reduction on control of fine particle nitrate, Atmospheric Chem. Phys., 18, 12241–12256, https://doi.org/10.5194/acp-18-12241-2018, 2018.

He, Y., Pan, Y., Zhang, G., Ji, D., Tian, S., Xu, X., Zhang, R., and Wang, Y.: Tracking ammonia morning peak, sources and transport with 1 Hz measurements at a rural site in North China Plain, Atmos Environ, 235, 117630, https://doi.org/10.1016/j.atmosenv.2020.117630, 2020.

Horvath, L., Fagerli, H., and Sutton, M. A.: Long-Term Record (1981—2005) of Ammonia and Ammonium Concentrations at K-Puszta Hungary and the Effect of Sulphur Dioxide Emission Change on Measured and Modelled Concentrations, in: Atmospheric Ammonia: Detecting emission changes and environmental impacts, edited by: Sutton, M. A., Reis, S., and Baker, S. M. H., Springer Netherlands, Dordrecht, 181–185, https://doi.org/10.1007/978-1-4020-9121-6_12, 2009.

Horváth, L. and Sutton, M. A.: Long-term record of ammonia and ammonium concentrations at K-puszta, Hungary, Atmos Environ, 32, 339–344, https://doi.org/10.1016/S1352-2310(97)00046-0, 1998.

Hu, G., Zhang, Y., Sun, J., Zhang, L., Shen, X., Lin, W., and Yang, Y.: Variability, formation and acidity of water-soluble ions in $PM_{2.5}$ in Beijing based on the semi-continuous observations, Atmos Res, 145–146, 1–11, https://doi.org/10.1016/j.atmosres.2014.03.014, 2014.

Huang, X., Song, Y., Li, M., Li, J., Huo, Q., Cai, X., Zhu, T., Hu, M., and Zhang, H.: A high-resolution ammonia emission inventory in China, Global Biogeochem Cy, 26, GB1030, https://doi.org/10.1029/2011gb004161, 2012.

Huang, X., Zhang, J., Zhang, W., Tang, G., and Wang, Y.: Atmospheric ammonia and its effect on $PM_{2.5}$ pollution in urban Chengdu, Sichuan Basin, China, Environ Pollut, 291, 118195, https://doi.org/10.1016/j.envpol.2021.118195, 2021.

Ju, X., Xing, G., Chen, X., Zhang, S., Zhang, L., Liu, X., Cui, Z., Yin, B., Christie, P., Zhu, Z., and Zhang, F.: Reducing environmental risk by improving N management in intensive Chinese agricultural systems, Proceedings of the National Academy of Sciences, 106, 3041–3046, https://doi.org/10.1073/pnas.0813417106, 2009.

Kang, Y., Liu, M., Song, Y., Huang, X., Yao, H., Cai, X., Zhang, H., Kang, L., Liu, X., Yan, X., He, H., Zhang, Q., Shao, M., and Zhu, T.: High-resolution ammonia emissions inventories in China from 1980 to 2012, Atmos Chem Phys, 16, 2043–2058, https://doi.org/10.5194/acp-16-2043-2016, 2016.

Karydis, V. A., Tsimpidi, A. P., Pozzer, A., and Lelieveld, J.: How alkaline compounds control atmospheric aerosol particle acidity, Atmospheric Chem. Phys., 21, 14983–15001, https://doi.org/10.5194/acp-21-14983-2021, 2021.

Lachatre, M., Fortems-Cheiney, A., Foret, G., Siour, G., Dufour, G., Clarisse, L., Clerbaux, C., Coheur, P.-F., Van Damme, M., and Beekmann, M.: The unintended consequence of SO2 and NO2 regulations over China: increase of ammonia levels and impact on $PM_{2.5}$ concentrations, Atmos Chem Phys, 19, 6701–6716, https://doi.org/10.5194/acp-19-6701-2019, 2019.

Lan, Z., Lin, W., Pu, W., and Ma, Z.: Measurement report: Exploring NH3 behavior in urban and suburban Beijing: comparison and implications, Atmos Chem Phys, 21, 4561–4573, https://doi.org/10.5194/acp-21-4561-2021, 2021.

Langford, A. O., Fehsenfeld, F. C., Zachariassen, J., and Schimel, D. S.: Gaseous ammonia fluxes and background concentrations in terrestrial ecosystems of the United States, Global Biogeochem Cy, 6, 459–483, https://doi.org/10.1029/92gb02123, 1992.

Li, Y., Schwandner, F. M., Sewell, H. J., Zivkovich, A., Tigges, M., Raja, S., Holcomb, S., Molenar, J. V., Sherman, L., Archuleta, C., Lee,

T., and Collett, J. L.: Observations of ammonia, nitric acid, and fine particles in a rural gas production region, Atmos Environ, 83, 80–89, https://doi.org/10.1016/j.atmosenv.2013.10.007, 2014.

Lin, W., Xu, X., Ge, B., and Liu, X.: Gaseous pollutants in Beijing urban area during the heating period 2007–2008: variability, sources, meteorological, and chemical impacts, Atmos Chem Phys, 11, 8157–8170, https://doi.org/10.5194/acp-11-8157-2011, 2011.

Liu, L., Zhang, X., Wong, A. Y. H., Xu, W., Liu, X., Li, Y., Mi, H., Lu, X., Zhao, L., Wang, Z., Wu, X., and Wei, J.: Estimating global surface ammonia concentrations inferred from satellite retrievals, Atmos Chem Phys, 19, 12051–12066, https://doi.org/10.5194/acp-19-12051-2019, 2019a.

Liu, M., Huang, X., Song, Y., Tang, J., Cao, J., Zhang, X., Zhang, Q., Wang, S., Xu, T., Kang, L., Cai, X., Zhang, H., Yang, F., Wang, H., Yu, J. Z., Lau, A. K. H., He, L., Huang, X., Duan, L., Ding, A., Xue, L., Gao, J., Liu, B., and Zhu, T.: Ammonia emission control in China would mitigate haze pollution and nitrogen deposition, but worsen acid rain, Proc. Natl. Acad. Sci., 116, 7760–7765, https://doi.org/10.1073/pnas.1814880116, 2019b.

Liu, M., Huang, X., Song, Y., Xu, T., Wang, S., Wu, Z., Hu, M., Zhang, L., Zhang, Q., Pan, Y., Liu, X., and Zhu, T.: Rapid SO_2 emission reductions significantly increase tropospheric ammonia concentrations over the North China Plain, Atmos Chem Phys, 18, 17933–17943, https://doi.org/10.5194/acp-18-17933-2018, 2018.

Liu, X., Pu, W., Ma, Z., Lin, W., Han, T., Li, Y., Zhou, L., and Shi, Q.: Study on the temporal and spatial variation of atmospheric ammonia in Beijing (China), China Environmental Science, 41, 3473–3483, https://doi.org/10.19674/j.cnki.issn1000-6923.20210426.001, 2021.

Lolkema, D. E., Noordijk, H., Stolk, A. P., Hoogerbrugge, R., van Zanten, M. C., and van Pul, W. A. J.: The Measuring Ammonia in Nature (MAN) network in the Netherlands, Biogeosciences, 12, 5133–5142, https://doi.org/10.5194/bg-12-5133-2015, 2015.

Luo, X., Liu, X., Pan, Y., Wen, Z., Xu, W., Zhang, L., Kou, C., Lv, J., and Goulding, K.: Atmospheric reactive nitrogen concentration and deposition trends from 2011 to 2018 at an urban site in north China, Atmos Environ, 224, 117298, https://doi.org/10.1016/j.atmosenv.2020.117298, 2020.

Luukko, P. J. J., Helske, J., and Räsänen, E.: Introducing libeemd: a program package for performing the ensemble empirical mode decomposition, Computation Stat, 31, 545–557, https://doi.org/10.1007/s00180-015-0603-9, 2016.

Meng, F., Zhang, Y., Kang, J., Heal, M. R., Reis, S., Wang, M., Liu, L., Wang, K., Yu, S., Li, P., Wei, J., Hou, Y., Zhang, Y., Liu, X., Cui, Z., Xu, W., and Zhang, F.: Trends in secondary inorganic aerosol pollution in China and its responses to emission controls of precursors in wintertime, Atmos Chem Phys, 22, 6291–6308, https://doi.org/10.5194/acp-22-6291-2022, 2022.

Meng, Z., Lin, W., Zhang, R., Han, Z., and Jia, X.: Summertime ambient ammonia and its effects on ammonium aerosol in urban Beijing, China, Science of The Total Environment, 579, 1521–1530, https://doi.org/10.1016/j.scitotenv.2016.11.159, 2017.

Nair, A. A. and Yu, F.: Quantification of Atmospheric Ammonia Concentrations: A Review of Its Measurement and Modeling, Atmosphere-basel, 11, 1092, https://doi.org/10.3390/atmos11101092, 2020.

Nguyen, D. V., Sato, H., Hamada, H., Yamaguchi, S., Hiraki, T., Nakatsubo, R., Murano, K., and Aikawa, M.: Symbolic seasonal variation newly found in atmospheric ammonia concentration in urban area of Japan, Atmos Environ, 244, 117943, https://doi.org/10.1016/j.atmosenv.2020.117943, 2021.

Olivier, J. G. J., Bouwman, A. F., Van der Hoek, K. W., and Berdowski, J. J. M.: Global air emission inventories for anthropogenic sources of NOx, NH3 and N2O in 1990, Environ. Pollut., 102, 135–148, https://doi.org/10.1016/S0269-7491(98)80026-2, 1998.

Pan, Y., Tian, S., Zhao, Y., Zhang, L., Zhu, X., Gao, J., Huang, W., Zhou, Y., Song, Y., Zhang, Q., and Wang, Y.: Identifying Ammonia Hotspots in China Using a National Observation Network, Environ Sci Technol, 52, 3926–3934,

https://doi.org/10.1021/acs.est.7b05235, 2018.

Park, J., Kim, E., Oh, S., Kim, H., Kim, S., Kim, Y. P., and Song, M.: Contributions of Ammonia to High Concentrations of PM2.5 in an Urban Area, Atmosphere-basel, 12, 1676, https://doi.org/10.3390/atmos12121676, 2021.

570   Perrino, C., Catrambone, M., Di Menno Di Bucchianico, A., and Allegrini, I.: Gaseous ammonia in the urban area of Rome, Italy and its relationship with traffic emissions, Atmos Environ, 36, 5385–5394, https://doi.org/10.1016/s1352-2310(02)00469-7, 2002.

Phan, N.-T., Kim, K.-H., Shon, Z.-H., Jeon, E.-C., Jung, K., and Kim, N.-J.: Analysis of ammonia variation in the urban atmosphere, Atmos Environ, 65, 177–185, https://doi.org/10.1016/j.atmosenv.2012.10.049, 2013.

Pinder, R. W., Gilliland, A. B., and Dennis, R. L.: Environmental impact of atmospheric NH3 emissions under present and future

575   conditions in the eastern United States, Geophys Res Lett, 35, L12808, https://doi.org/10.1029/2008gl033732, 2008.

Pu, W., Ma, Z., Collett Jr, J. L., Guo, H., Lin, W., Cheng, Y., Quan, W., Li, Y., Dong, F., and He, D.: Regional transport and urban emissions are important ammonia contributors in Beijing, China, Environ Pollut, 265, 115062, https://doi.org/10.1016/j.envpol.2020.115062, 2020.

Qian, C., Fu, C., and Wu, Z.: Changes in the Amplitude of the Temperature Annual Cycle in China and Their Implication for Climate

580   Change Research, J Climate, 24, 5292–5302, https://doi.org/10.1175/JCLI-D-11-00006.1, 2011.

Reay, D. S., Dentener, F., Smith, P., Grace, J., and Feely, R. A.: Global nitrogen deposition and carbon sinks, Nat Geosci, 1, 430–437, https://doi.org/10.1038/ngeo230, 2008.

Saraswati, George, M. P., Sharma, S. K., Mandal, T. K., and Kotnala, R. K.: Simultaneous Measurements of Ambient NH3 and Its Relationship with Other Trace Gases, PM2.5 and Meteorological Parameters over Delhi, India, MAPAN, 34, 55–69,

585   https://doi.org/10.1007/s12647-018-0286-0, 2019.

Saraswati, Sharma, S. K., and Mandal, T. K.: Five-year measurements of ambient ammonia and its relationships with other trace gases at an urban site of Delhi, India, Meteorol Atmos Phys, 130, 241–257, https://doi.org/10.1007/s00703-017-0512-2, 2017.

Shadman, S., Rose, C., and Yalin, A. P.: Open-path cavity ring-down spectroscopy sensor for atmospheric ammonia, Applied Physics B, 122, 194, https://doi.org/10.1007/s00340-016-6461-5, 2016.

590   Sharma, S. K., Mandal, T. K., Sharma, C., Kuniyal, J. C., Joshi, R., Dhyani, P. P., Rohtash, Sen, A., Ghayas, H., Gupta, N. C., Sharma, P., Saxena, M., Sharma, A., Arya, B. C., and Kumar, A.: Measurements of Particulate (PM2.5), BC and Trace Gases Over the Northwestern Himalayan Region of India, MAPAN, 29, 243–253, https://doi.org/10.1007/s12647-014-0104-2, 2014.

Shon, Z.-H., Kim, K.-H., Song, S.-K., Jung, K., Kim, N.-J., and Lee, J.-B.: Relationship between water-soluble ions in PM2.5 and their precursor gases in Seoul megacity, Atmos Environ, 59, 540–550, https://doi.org/10.1016/j.atmosenv.2012.04.033, 2012.

595   Singh, S. and Kulshrestha, U. C.: Rural versus urban gaseous inorganic reactive nitrogen in the Indo-Gangetic plains (IGP) of India, Environ Res Lett, 9, 125004, https://doi.org/10.1088/1748-9326/9/12/125004, 2014.

Sun, Q., Gu, M., Wu, D., Yang, T., Wang, H., and Pan, Y.: Concurrent measurements of atmospheric ammonia concentrations in the megacities of Beijing and Shanghai by using cavity ring-down spectroscopy, Atmos Environ, 307, 119848, https://doi.org/10.1016/j.atmosenv.2023.119848, 2023.

600   Sutton, M. A., Tang, Y. S., Dragosits, U., Fournier, N., Dore, A. J., Smith, R. I., Weston, K. J., and Fowler, D.: A spatial analysis of atmospheric ammonia and ammonium in the U.K, ScientificWorldJournal, 1 Suppl 2, 275–286, https://doi.org/10.1100/tsw.2001.313, 2001.

Tang, Y. S., Braban, C. F., Dragosits, U., Dore, A. J., Simmons, I., van Dijk, N., Poskitt, J., Dos Santos Pereira, G., Keenan, P. O., Conolly, C., Vincent, K., Smith, R. I., Heal, M. R., and Sutton, M. A.: Drivers for spatial, temporal and long-term trends in atmospheric

ammonia and ammonium in the UK, Atmos Chem Phys, 18, 705–733, https://doi.org/10.5194/acp-18-705-2018, 2018.

Teng, X., Hu, Q., Zhang, L., Qi, J., Shi, J., Xie, H., Gao, H., and Yao, X.: Identification of Major Sources of Atmospheric NH3in an Urban Environment in Northern China During Wintertime, Environ. Sci. Technol., 51, 6839–6848, https://doi.org/10.1021/acs.est.7b00328, 2017.

Van Damme, M., Clarisse, L., Whitburn, S., Hadji-Lazaro, J., Hurtmans, D., Clerbaux, C., and Coheur, P.-F.: Industrial and agricultural ammonia point sources exposed, Nature, 564, 99–103, https://doi.org/10.1038/s41586-018-0747-1, 2018.

Van Damme, M., Whitburn, S., Clarisse, L., Clerbaux, C., Hurtmans, D., and Coheur, P.-F.: Version 2 of the IASI NH₃ neural network retrieval algorithm: near-real-time and reanalysed datasets, Atmos Meas Tech, 10, 4905–4914, https://doi.org/10.5194/amt-10-4905-2017, 2017.

Vu, T. V., Shi, Z., Cheng, J., Zhang, Q., He, K., Wang, S., and Harrison, R. M.: Assessing the impact of clean air action on air quality trends in Beijing using a machine learning technique, Atmos Chem Phys, 19, 11303–11314, https://doi.org/10.5194/acp-19-11303-2019, 2019.

Walters, W. W., Karod, M., Willcocks, E., Baek, B. H., Blum, D. E., and Hastings, M. G.: Quantifying the importance of vehicle ammonia emissions in an urban area of northeastern USA utilizing nitrogen isotopes, Atmospheric Chem. Phys., 22, 13431–13448, https://doi.org/10.5194/acp-22-13431-2022, 2022.

Wang, H. and Zhang, L.: Trends of inorganic sulfur and nitrogen species at an urban site in western Canada (2004–2018), Environ. Pollut., 333, 122079, https://doi.org/10.1016/j.envpol.2023.122079, 2023.

Wang, H., Zhang, L., Yao, X., Cheng, I., and Dabek-Zlotorzynska, E.: Identification of decadal trends and associated causes for organic and elemental carbon in PM2.5 at Canadian urban sites, Environ. Int., 159, 107031, https://doi.org/10.1016/j.envint.2021.107031, 2022.

Wang, Q., Zhang, Q., Ma, Z., Ge, B., Xie, C., Zhou, W., Zhao, J., Xu, W., Du, W., Fu, P., Lee, J., Nemitz, E., Cowan, N., Mullinger, N., Cheng, X., Zhou, L., Yue, S., Wang, Z., and Sun, Y.: Temporal characteristics and vertical distribution of atmospheric ammonia and ammonium in winter in Beijing, Science of The Total Environment, 681, 226–234, https://doi.org/10.1016/j.scitotenv.2019.05.137, 2019.

Wang, R., Ye, X., Liu, Y., Li, H., Yang, X., Chen, J., Gao, W., and Yin, Z.: Characteristics of atmospheric ammonia and its relationship with vehicle emissions in a megacity in China, Atmos Environ, 182, 97–104, https://doi.org/10.1016/j.atmosenv.2018.03.047, 2018.

Wang, S., Nan, J., Shi, C., Fu, Q., Gao, S., Wang, D., Cui, H., Saiz-Lopez, A., and Zhou, B.: Atmospheric ammonia and its impacts on regional air quality over the megacity of Shanghai, China, Sci Rep-uk, 5, 15842, https://doi.org/10.1038/srep15842, 2015.

Warner, J. X., Dickerson, R. R., Wei, Z., Strow, L. L., Wang, Y., and Liang, Q.: Increased atmospheric ammonia over the world's major agricultural areas detected from space, Geophys. Res. Lett., 44, 2875–2884, https://doi.org/10.1002/2016gl072305, 2017.

Wei, J., Li, Z., Chen, X., Li, C., Sun, Y., Wang, J., Lyapustin, A., Brasseur, G. P., Jiang, M., Sun, L., Wang, T., Jung, C. H., Qiu, B., Fang, C., Liu, X., Hao, J., Wang, Y., Zhan, M., Song, X., and Liu, Y.: Separating Daily 1 km PM2.5 Inorganic Chemical Composition in China since 2000 via Deep Learning Integrating Ground, Satellite, and Model Data, Environ Sci Technol, 57, 13025–13035, https://doi.org/10.1021/acs.est.3c00272, 2023.

Wei, Z. and Mohamed Tahrin, N.: Impact of Gaseous Pollutants Reduction on Fine Particulate Matter and Its Secondary Inorganic Aerosols in Beijing–Tianjin–Hebei Region, Atmosphere, 14, 1027, https://doi.org/10.3390/atmos14061027, 2023.

Wen, Z., Ma, X., Xu, W., Si, R., Liu, L., Ma, M., Zhao, Y., Tang, A., Zhang, Y., Wang, K., Zhang, Y., Shen, J., Zhang, L., Zhao, Y., Zhang, F., Goulding, K., and Liu, X.: Combined short-term and long-term emission controls improve air quality sustainably in China, Nat.

Commun., 15, 5169, https://doi.org/10.1038/s41467-024-49539-9, 2024.

Wen, Z., Xu, W., Li, Q., Han, M., Tang, A., Zhang, Y., Luo, X., Shen, J., Wang, W., Li, K., Pan, Y., Zhang, L., Li, W., Collett, J. L., Zhong, B., Wang, X., Goulding, K., Zhang, F., and Liu, X.: Changes of nitrogen deposition in China from 1980 to 2018, Environ Int, 144, 106022, https://doi.org/10.1016/j.envint.2020.106022, 2020.

Wentworth, G. R., Murphy, J. G., Benedict, K. B., Bangs, E. J., and Collett Jr., J. L.: The role of dew as a night-time reservoir and morning source for atmospheric ammonia, Atmospheric Chem. Phys., 16, 7435–7449, https://doi.org/10.5194/acp-16-7435-2016, 2016.

Wu, L., Sun, J., Zhang, X., Zhang, Y., Wang, Y., Zhong, J., and Yang, Y.: Aqueous-phase reactions occurred in the PM2.5 cumulative explosive growth during the heavy pollution episode (HPE) in 2016 Beijing wintertime, Tellus B: Chemical and Physical Meteorology, 71, 1620079, https://doi.org/10.1080/16000889.2019.1620079, 2019.

Wu, Z. and Huang, N. E.: Ensemble empirical mode decomposition: a noise-assisted data analysis method, Adv. Adapt. Data Anal., 01, 1–41, https://doi.org/10.1142/S1793536909000047, 2009.

Xie, X., Hu, J., Qin, M., Guo, S., Hu, M., Wang, H., Lou, S., Li, J., Sun, J., Li, X., Sheng, L., Zhu, J., Chen, G., Yin, J., Fu, W., Huang, C., and Zhang, Y.: Modeling particulate nitrate in China: Current findings and future directions, Environ Int, 166, 107369, https://doi.org/10.1016/j.envint.2022.107369, 2022.

Xu, J., Lu, M., Guo, Y., Zhang, L., Chen, Y., Liu, Z., Zhou, M., Lin, W., Pu, W., Ma, Z., Song, Y., Pan, Y., Liu, L., and Ji, D.: Summertime Urban Ammonia Emissions May Be Substantially Underestimated in Beijing, China, Environ. Sci. Technol., 57, 13124–13135, https://doi.org/10.1021/acs.est.3c05266, 2023.

Xu, W., Zhang, L., and Liu, X.: A database of atmospheric nitrogen concentration and deposition from the nationwide monitoring network in China, Sci Data, 6, https://doi.org/10.1038/s41597-019-0061-2, 2019.

Yamamoto, N., Kabeya, N., Onodera, M., Takahahi, S., Komori, Y., Nakazuka, E., and Shirai, T.: Seasonal variation of atmospheric ammonia and particulate ammonium concentrations in the urban atmosphere of yokohama over a 5-year period, Atmos Environ, 22, 2621–2623, https://doi.org/10.1016/0004-6981(88)90498-2, 1988.

Yamamoto, N., Nishiura, H., Honjo, T., Ishikawa, Y., and Suzuki, K.: A long-term study of atmospheric ammonia and particulate ammonium concentrations in Yokohama, Japan, Atmos Environ, 29, 97–103, https://doi.org/10.1016/1352-2310(94)00226-b, 1995.

Yamanouchi, S., Viatte, C., Strong, K., Lutsch, E., Jones, D. B. A., Clerbaux, C., Van Damme, M., Clarisse, L., and Coheur, P.-F.: Multiscale observations of NH3 around Toronto, Canada, Atmos Meas Tech, 14, 905–921, https://doi.org/10.5194/amt-14-905-2021, 2021.

Yao, X., Hu, Q., Zhang, L., Evans, G. J., Godri, K. J., and Ng, A. C.: Is vehicular emission a significant contributor to ammonia in the urban atmosphere?, Atmos. Environ., 80, 499–506, https://doi.org/10.1016/j.atmosenv.2013.08.028, 2013.

Yao, X. and Zhang, L.: Trends in atmospheric ammonia at urban, rural, and remote sites across North America, Atmospheric Chem. Phys., 16, 11465–11475, https://doi.org/10.5194/acp-16-11465-2016, 2016.

Yao, X. and Zhang, L.: Causes of Large Increases in Atmospheric Ammonia in the Last Decade across North America, ACS Omega, 4, 22133–22142, https://doi.org/10.1021/acsomega.9b03284, 2019.

Yu, F., Nair, A. A., and Luo, G.: Long-Term Trend of Gaseous Ammonia Over the United States: Modeling and Comparison With Observations, J Geophys Res-atmos, 123, 8315–8325, https://doi.org/10.1029/2018JD028412, 2018.

Zbieranowski, A. L. and Aherne, J.: Ambient concentrations of atmospheric ammonia, nitrogen dioxide and nitric acid across a rural–urban–agricultural transect in southern Ontario, Canada, Atmos Environ, 62, 481–491, https://doi.org/10.1016/j.atmosenv.2012.08.040, 2012.

Zhang, X., Lin, W., Ma, Z., and Xu, X.: Indoor NH_3 variation and its relationship with outdoor NH3 in urban Beijing, Indoor Air, 31, 2130–2141, https://doi.org/10.1111/ina.12907, 2021.

Zhang, Y., Benedict, K. B., Tang, A., Sun, Y., Fang, Y., and Liu, X.: Persistent Nonagricultural and Periodic Agricultural Emissions Dominate Sources of Ammonia in Urban Beijing: Evidence from 15N Stable Isotope in Vertical Profiles, Environ Sci Technol, 54, 102–109, https://doi.org/10.1021/acs.est.9b05741, 2019.

Zhang, Y., Liu, X., Fang, Y., Liu, D., Tang, A., and Collett, J. L.: Atmospheric Ammonia in Beijing during the COVID-19 Outbreak: Concentrations, Sources, and Implications, Environ Sci Tech Let, 8, 32–38, https://doi.org/10.1021/acs.estlett.0c00756, 2020.

Zheng, M., Wang, Y., Yuan, L., Chen, N., and Kong, S.: Ambient observations indicating an increasing effectiveness of ammonia control in wintertime $PM_{2.5}$ reduction in Central China, Science of The Total Environment, 824, 153708, https://doi.org/10.1016/j.scitotenv.2022.153708, 2022.

Zhou, C., Zhou, H., Holsen, T. M., Hopke, P. K., Edgerton, E. S., and Schwab, J. J.: Ambient Ammonia Concentrations Across New York State, J Geophys Res-atmos, 124, 8287–8302, https://doi.org/10.1029/2019jd030380, 2019.

Zhou, Y., Shuiyuan Cheng, Lang, J., Chen, D., Zhao, B., Liu, C., Xu, R., and Li, T.: A comprehensive ammonia emission inventory with high-resolution and its evaluation in the Beijing–Tianjin–Hebei (BTH) region, China, Atmos. Environ., 106, 305–317, https://doi.org/10.1016/j.atmosenv.2015.01.069, 2015.